VFAST Transactions on Mathematics
http://vfast.org/journals/index.php/VTM@ 2021, ISSN(e): 2309-0022, ISSN(p): 2411-6343
Volume 10, Number 2, July-December, 2022 *pp: 21-33*

Analytical Solution of Transient Flow of Fractional Oldroyd-B Fluid between Oscillating Cylinders

Khadija Shaikh[1*], Fozia Shaikh[1], Syed Feroz Shah[1], Rahim Bux Khokhar[1], K.N. Memon[2]

[1] Department of Basic Sciences and Related Studies, Mehran University of Engineering and Technology, Jamshoro , Sindh, Pakistan; [2]Department of Mathematics and Statistics, Quaid-e-Awaam University of Engineering, Science and Technology, Nawabshah , Sindh, Pakistan.

Keywords: *Fractional Oldroyd-B fluid, Caputo fractional derivative, Integral transforms, Analytical solutions, Oscillating pressure gradient.* ***Subject Classification***: *Computational Fluid Dynamics, Fractional Calculus.*

Journal Info:
Submitted:
October 15 , 2022
Accepted:
November 05, 2022
Published:
November 12, 2022

Abstract This paper investigates the fractional Oldroyd-B fluid flow across two interminable coaxial cylinders, where the fluid's motion is generated by the oscillatory movement of cylinders and the oscillating pressure gradient. The profile of velocity and shear stress of the flow is derived with the assistance of Caputo fractional derivative utilizing a analytical technique, finite Hankel transform and Laplace transforms. The semi-analytical solution is then displayed as generalized functions of G and R satisfying fundamental constitutive equations and all initial and boundary conditions. To validate the results, some limitations have been imposed on the determined equations and the results have been contrasted against previous results. Moreover, the influence of various parameters on the flow of fractionalized Oldroyd-B fluid is investigated and depicted graphically.

***Correspondence Author Email Address:**
khadijadoqadir@gmail.com

1 Introduction

Non-Newtonian fluids are an immensely employed fluid across the world; used across lengths and breadths of research in medicine, industries and engineering, scholars posit special curiosity towards the subject. The researchers, including [25] and [21] have investigated the subject of Oldroyd-B fluid's motion; courtesy of its extensive employment in engineering craft, the most renowned among the family of non-Newtonian rate-type fluids. A thorough analysis, concerning the time-dependence of viscous Maxwell fluid's motions across two oscillating coaxial cylinders, where the outer cylinder is retained immobilized while utilizing integral transform has also been done by [9]. Further, some work has also been undertaken by [2] on the unsteady movement of Generalized Maxwell fluids between two infinite horizontal cylinders. A longitudinal and torsional investigation has also been instituted on conclusions derived - employing Hankel and Laplace transforms – vis-a-vis behaviour postulated by second-grade fluid among cylinders [5]. The rise in industrial applications of oscillating cylindrical geometries in the consumer market has given rise to increased interest by research and development scientists across the technological world. In these circumstances, an extensive appraisal of the generalized Maxwell liquid's torsional oscillatory motion in between two coaxial cylinders of circular shape is given in [23]. Some common examples of the same are pneumatic valves, hydraulic valves and cylinder engines etc. On account of non-Newtonian fluid's non-linear behaviour, it becomes pertinent to adopt various numerical and analytical approaches [19],[18],[13],[1],[10]. Among the assortment of methods available for deriving solutions to such problems, fractional calculus is the most celebrated. Originally introduced for application upon viscous-diffusion fluid mechanics systems constrained in bounds of time, the modern era has expanded this technique's approach to non-linear motion problems as well; this, resultantly, not only gives solutions akin to the classical methods but also provides researchers with history too. Making use of time-constrained fractional Caputo derivative, the works of [16] explore the behaviour of fractional Maxwell fluids in rectangular channels. Some of the most famously used fractional derivatives, as described in [20], [24], are Riemann-Liouville, Atangana-Baleanu, Caputo and Fabrizio, Caputo-Liouville, and Caputo. This study resolves to administer Caputo fractional derivatives for the derivation of analytical results of the shear stress and velocity profile, in the presence of an oscillating pressure gradient, of an oscillating coaxial cylinder housing Oldroyd-B fluid.

2 Formulation of the Problem

Supposing that incompressible Oldroyd-B fluid between two interminable coaxial cylinders, having radii R_1 and R_2 ($R_2 > R_1$), as provided below in Fig. 1 inspired by [9]. In this hypothetical situation, we assume the coordinates of the cylinder as (r, θ, z), while keeping the r-axis and z-axis perpendicular and along the cylinder respectively.

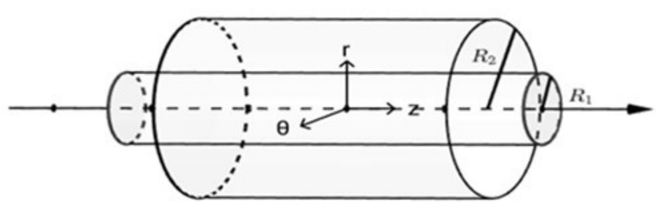

Figure 1. Problem Geometry [9]

Originally, cylinders are at a stationary position, whereas when an external time-dependent oscillating pressure gradient is applied to the subject's body, we observe movement in the fluid present inside the body. The direction of flow in this circumstance is observed in θ–direction, however, the cylinders oscillate accompanying their common axis.

3 Basic Governing Equations

When gravitational force is ignored in the scenario, the equations that regulate the flow of incompressible Oldroyd-B fluid are provided in [3]:

$$\nabla \cdot \overline{V} = 0 \tag{1}$$

$$\rho \frac{D\overline{V}}{Dt} = \nabla \cdot \overline{\mathrm{T}} \tag{2}$$

The velocity vector is signified by $\overline{V}$, the constant density of the fluid is given as ρ, while $\overline{\mathrm{T}}$ denotes the Cauchy stress tensor. Relevant equations pertinent to the defined flow of Oldroyd-B fluid receive mention in [3]:

$$\overline{\mathrm{T}} = p\overline{\mathrm{I}} + \overline{\mathrm{S}}, \overline{\mathrm{S}} + \lambda \left[\frac{\partial \overline{\mathrm{S}}}{\partial t} + (\overline{\mathrm{V}} \cdot \nabla)\overline{\mathrm{S}} - (\nabla\overline{V})\overline{\mathrm{S}} - \overline{\mathrm{S}}(\nabla\overline{V}^T)\right] = \mu\left\{\overline{\mathrm{A}} + \lambda_r \left[\frac{\partial \overline{\mathrm{A}}}{\partial t} + (\overline{\mathrm{V}} \cdot \nabla)\overline{\mathrm{A}} - (\nabla\overline{V})\overline{\mathrm{A}} - \overline{\mathrm{A}}(\nabla\overline{V}^T)\right]\right\} \tag{3}$$

In this scenario, the unit tensor is indicated by I, L stands for velocity gradient (per second), $\overline{S}$ signals extra-stress tensor (with SI unit fixed at Newton per meter^2), μ designates dynamic velocity (Newton second per meter^2), p signalling pressure (with Pascal as SI unit), while λ marks relaxation parameter and retardation parameter identifies $\lambda_r(0 \leq \lambda_r < \lambda)$. The rate of deformation is provided as $\overline{A} = \nabla\overline{V} + \nabla\overline{V}^T$. When the ordinary differential operator is replaced by the fractional differential operator, eq. $(3)_2$ becomes as follows [14], [6]:

$$\overline{\mathrm{S}} + \lambda\left[D_t^{\alpha}\overline{\mathrm{S}} + (\overline{\mathrm{V}} \cdot \nabla)\overline{\mathrm{S}} - \overline{\mathrm{LS}} - \overline{\mathrm{SL}}^T\right] = \mu\left\{\overline{\mathrm{A}} + \lambda_r\left[D_t^{\alpha}\overline{\mathrm{A}} + (\overline{\mathrm{V}} \cdot \nabla)\overline{\mathrm{A}} - \overline{\mathrm{LA}} - \overline{\mathrm{AL}}^T\right]\right\} \tag{4}$$

In this scenario, Caputo fractional differential operator is defined as D_t^{α} in [15]:

$$D_t^{\alpha}h(t) = \begin{cases} \frac{1}{\Gamma(1-\alpha)}\frac{d}{dt}\int_0^t \frac{h(x)}{(t-x)^{\alpha}}dx & 0 < \alpha < 1 \\ \frac{dh(t)}{dt} & \alpha = 1 \end{cases} \tag{5}$$

In the study undertaken presently, the motion has extra-stress $\overline{S}$ and velocity field $\overline{V}$ as in [23]:

$$\overline{V} = v(r,t)e_{\theta}, \quad \overline{S} = S(r,t) \tag{6}$$

Thus, motion's direction within the cylindrical coordinate system of r, z and θ is indicated by e_{θ}. In every corresponding flow of this sort, identical satisfaction exists in the continuity equation. As, both the geometry and fluid are stationary at first, therefore the value of time is equal to zero, i.e

$$\overline{V}(r,0) = 0 \text{ and } \overline{S}(r,0) = 0 \tag{7}$$

However, motion in θ-direction in the inner cylinder is observed as soon as t becomes 0^+, on account of administered time-dependent pressure gradient, i.e:

$$\frac{\partial p}{\partial \theta} = -\rho p_0 \sin \omega t \tag{8}$$

Substituting eq.(6) in eq.(4) and (7)-(8), resultant mathematical model appears:

$$(1 + \lambda D_t^{\alpha})\tau(r,t) = \mu(1 + \lambda_r D_t^{\alpha})\left(\frac{\partial}{\partial r} - \frac{1}{r}\right)v(r,t) \tag{9}$$

$$(1 + \lambda D_t^{\alpha})\frac{\partial v(r,t)}{\partial t} + \frac{1}{\rho r}(1 + \lambda D_t^{\alpha})\frac{\partial P}{\partial \theta} = \nu(1 + \lambda_r D_t^{\delta})\left(\frac{\partial^2}{\partial r^2} + \frac{1}{r}\frac{\partial}{\partial r} + \frac{1}{r^2}\right)v(r,t) \tag{10}$$

The non-trivial shear stress is $\tau(r,t) = S_{r\theta}(r,t)$, the kinematic viscosity is $\nu = \frac{\mu}{\rho}$ fractional parameters are identified as α and δ, in a manner so that, $0 \leq \delta \leq \alpha \leq 1$. Hence, the corresponding conditions (boundary and initial) are:

$$v(r,0) = \frac{\partial v(r,0)}{\partial t} = 0 \tag{11}$$

$$v(R_1,t) = \omega_1 \sin \beta_1 t \text{ and } v(R_2,t) = \omega_2 \sin \beta_2 t \tag{12}$$

Where the amplitudes are notified by ω_1, ω_2 while respective cylinders' frequencies are defined as β_1, β_2 and $r \in (R_1, R_2)$.

4 Velocity Profile

Plugging the Laplace transform defined in [4] on eq.(10) and (12), the following equation is achieved:

$$(s + \lambda s^{\alpha+1})\overline{v}(r,s) - \frac{1}{r}(1 + \lambda s^{\alpha})\frac{P_0\omega}{s^2+\omega^2} = \nu(1+\lambda_r s^{\delta})\left(\frac{\partial^2}{\partial r^2} + \frac{1}{r}\frac{\partial}{\partial r} + \frac{1}{r^2}\right)\overline{v}(r,s) \tag{13}$$

$$\overline{v}(R_1,s)\frac{\omega_1\beta_1}{s^2+\beta_1^2} \text{ and } \overline{v}(R_1,s)\frac{\omega_2\beta_2}{s^2+\beta_2^2} \tag{14}$$

The finite Hankel transform is defined as [21]:

$$H_n\{f(r)\} = \tilde{f}(\kappa_\gamma) = \int_a^b rf(r)A_n(r\kappa_\gamma)dr, \qquad b > a \tag{15}$$

Where, $A_n(r\kappa_\gamma) = J_n(r\kappa_\gamma)Y_n(a\kappa_\gamma) - Y_n(r\kappa_\gamma)J_n(a\kappa_\gamma)$.
Here positive roots of $A_n(r\kappa_\gamma) = 0$ are denoted by κ_γ, while the first and second types of Bessel functions of order n are signified, respectively, by $J_n(.)$ and $Y_n(.)$, respectively. In this case, when we make use of $rA_n(r\kappa_\gamma)$ in Eq. (13) as well as integration, it brings us to:

$$\begin{aligned}\overline{v}_H(\kappa_\gamma,s) = &\left[\frac{2}{\pi}\frac{\omega_2\beta_2}{s^2+\beta_2^2} - \frac{2}{\pi}\frac{\omega_1\beta_1}{s^2+\beta_1^2}\frac{J_1(R_2\kappa_\gamma)}{J_1(R_1\kappa_\gamma}\right] \times \frac{\nu(1+\lambda_r s^{\delta})}{s+\lambda s^{\alpha+1}+\kappa_\gamma^2\nu+\kappa_\gamma^2\nu\lambda_r s^{\delta}} \\ &+ \frac{P_0\omega(1+\lambda s^{\alpha})[\overline{A_1}(R_1\kappa_\gamma) - \overline{A_1}(R_2\kappa_\gamma)]}{\kappa_\gamma(s^2+\omega^2)} \times \frac{1}{s+\lambda s^{\alpha+1}+\kappa_\gamma^2\nu+\kappa_\gamma^2\nu\lambda_r s^{\delta}}\end{aligned} \tag{16}$$

Where, $\overline{A}_1(r\kappa_\gamma) = J_0(r\kappa_\gamma)Y_1(R_2\kappa_\gamma) - J_1(R_2\kappa_\gamma)Y_0(r\kappa_\gamma)$ is given in [22]:
The eq.(16) can be written in a suitable form as follows:

$$\begin{aligned}\overline{v}_H(\kappa_\gamma,s) = &\frac{2}{\pi\kappa_\gamma^2}\frac{\omega_2\beta_2}{s^2+\beta_2^2} - \frac{2}{\pi\kappa_\gamma^2}\frac{\omega_1\beta_1}{s^2+\beta_1^2}\frac{J_1(R_2\kappa_\gamma)}{J_1(R_1\kappa_\gamma} - \left[\frac{2}{\pi\kappa_\gamma^2}\frac{\omega_2\beta_2}{s^2+\beta_2^2} - \frac{2}{\pi\kappa_\gamma^2}\frac{\omega_1\beta_1}{s^2+\beta_1^2}\frac{J_1(R_2\kappa_\gamma)}{J_1(R_1\kappa_\gamma}\right] \\ &\times \frac{s+\lambda s^{\alpha+1}}{s+\lambda s^{\alpha+1}+\kappa_\gamma^2\nu+\kappa_\gamma^2\nu\lambda_r s^{\delta}} + \frac{P_0\omega[\overline{A_1}(R_1\kappa_\gamma) - \overline{A_1}(R_2\kappa_\gamma)]}{\kappa_\gamma(s^2+\omega^2)} \\ &\times \frac{1+\lambda s^{\alpha}}{s+\lambda s^{\alpha+1}+\kappa_\gamma^2\nu+\kappa_\gamma^2\nu\lambda_r s^{\delta}}\end{aligned} \tag{17}$$

The Inverse Hankel transform is defined as [4]:

$$\overline{v}(r,s) = \frac{\pi^2}{2}\sum_{\gamma=1}^{\infty}\frac{\kappa_\gamma^2 J_1^2(R_1\kappa_\gamma)A_1(r\kappa_\gamma)}{J_1^2(R_1\kappa_\gamma) - J_1^2(R_2\kappa_\gamma)}\overline{v}_H(\kappa_\gamma,s) \tag{18}$$

Employing Inverse Laplace transform on eq.(17) using eq. (18) and the following property:

$$\frac{R_2(r^2-R_1^2)}{(R_2^2-R_1^2)r} = \pi \sum_{\gamma=1}^{\infty} \frac{J_1^2(R_1\kappa_\gamma)A_1(r\kappa_\gamma)}{J_1^2(R_1\kappa_\gamma)-J_1^2(R_2\kappa_\gamma)} \tag{19}$$

The equation obtained is:

$$\begin{aligned}\bar{v}(r,s) =& \frac{\frac{\omega_1\beta_1}{s^2+\beta_1^2}R_1(R_2^2-r^2)+\frac{\omega_2\beta_2}{s^2+\beta_2^2}R_2(r^2-R_1^2)}{(R_2^2-R_1^2)r} \\ &+\pi\sum_{\gamma=1}^{\infty}\frac{J_1^2(R_1\kappa_\gamma)A_1(r\kappa_\gamma)}{J_1^2(R_1\kappa_\gamma)-J_1^2(R_2\kappa_\gamma)}\frac{\omega_1\beta_1(s+\lambda s^{\alpha+1})}{(s^2+\beta_1^2)(s+\lambda s^{\alpha+1}+\kappa_\gamma^2\nu+\kappa_\gamma^2\nu\lambda_r s^\delta)}\frac{J_1(R_2\kappa_\gamma)}{J_1(R_1\kappa_\gamma)} \\ &-\pi\sum_{\gamma=1}^{\infty}\frac{J_1^2(R_1\kappa_\gamma)A_1(r\kappa_\gamma)}{J_1^2(R_1\kappa_\gamma)-J_1^2(R_2\kappa_\gamma)}\frac{\omega_2\beta_2(s+\lambda s^{\alpha+1})}{(s^2+\beta_2^2)(s+\lambda s^{\alpha+1}+\kappa_\gamma^2\nu+\kappa_\gamma^2\nu\lambda_r s^\delta)} \\ &+\frac{\pi^2}{2}\sum_{\gamma=1}^{\infty}\frac{\kappa_\gamma J_1^2(R_1\kappa_\gamma)A_1(r\kappa_\gamma)}{J_1^2(R_1\kappa_\gamma)-J_1^2(R_2\kappa_\gamma)}\frac{P_0\omega(1+\lambda s^\alpha)[\overline{A_1}(R_1\kappa_\gamma)-\overline{A_1}(R_2\kappa_\gamma)]}{(s^2+\omega^2)} \\ &\times\frac{1}{s+\lambda s^{\alpha+1}+\kappa_\gamma^2\nu+\kappa_\gamma^2\nu\lambda_r s^\delta}\end{aligned} \tag{20}$$

Using the following identity [7]:

$$\frac{1}{s+\lambda s^{\alpha+1}+\kappa_\gamma^2\nu+\kappa_\gamma^2\nu\lambda_r s^\delta} = \frac{1}{\lambda}\sum_{i=0}^{\infty}\sum_{q=0}^{i}\frac{i!}{q!(i-q)!}\left(-\frac{\nu\kappa_\gamma^2}{\lambda}\right)^i\lambda_r^q\frac{s^{\delta q-i-1}}{(s^\alpha+\lambda^{-1})^{i+1}} \tag{21}$$

The eq.(20) takes the form:

$$\begin{aligned}\bar{v}(r,s) =& \frac{\frac{\omega_1\beta_1}{s^2+\beta_1^2}R_1(R_2^2-r^2)+\frac{\omega_2\beta_2}{s^2+\beta_2^2}R_2(r^2-R_1^2)}{(R_2^2-R_1^2)r} \\ &+\pi\sum_{\gamma=1}^{\infty}\frac{J_1^2(R_1\kappa_\gamma)A_1(r\kappa_\gamma)}{J_1^2(R_1\kappa_\gamma)-J_1^2(R_2\kappa_\gamma)}\frac{\omega_1\beta_1}{s^2+\beta_1^2}\frac{J_1(R_2\kappa_\gamma)}{J_1(R_1\kappa_\gamma)} \\ &\times\frac{1}{\lambda}\sum_{i=0}^{\infty}\sum_{q=0}^{i}\frac{i!}{q!(i-q)!}\left(-\frac{\nu\kappa_\gamma^2}{\lambda}\right)^i\lambda_r^q\frac{s^{\delta q-i}+\lambda s^{\delta q+\alpha-i}}{(s^\alpha+\lambda^{-1})^{i+1}} \\ &-\pi\sum_{\gamma=1}^{\infty}\frac{J_1^2(R_1\kappa_\gamma)A_1(r\kappa_\gamma)}{J_1^2(R_1\kappa_\gamma)-J_1^2(R_2\kappa_\gamma)}\frac{\omega_2\beta_2}{s^2+\beta_2^2}\times\frac{1}{\lambda}\sum_{i=0}^{\infty}\sum_{q=0}^{i}\frac{i!}{q!(i-q)!}\left(-\frac{\nu\kappa_\gamma^2}{\lambda}\right)^i\lambda_r^q\frac{s^{\delta q-i}+\lambda s^{\delta q+\alpha-i}}{(s^\alpha+\lambda^{-1})^{i+1}}+ \\ &\frac{\pi^2}{2}\sum_{\gamma=1}^{\infty}\frac{\kappa_\gamma J_1^2(R_1\kappa_\gamma)A_1(r\kappa_\gamma)}{J_1^2(R_1\kappa_\gamma)-J_1^2(R_2\kappa_\gamma)}\frac{P_0\omega[\overline{A_1}(R_1\kappa_\gamma)-\overline{A_1}(R_2\kappa_\gamma)]}{(s^2+\omega^2)} \\ &\times\frac{1}{\lambda}\sum_{i=0}^{\infty}\sum_{q=0}^{i}\frac{i!}{q!(i-q)!}\left(-\frac{\nu\kappa_\gamma^2}{\lambda}\right)^i\lambda_r^q\frac{s^{\delta q-i-1}+\lambda s^{\delta q+\alpha-i-1}}{(s^\alpha+\lambda^{-1})^{i+1}}\end{aligned} \tag{22}$$

Finally, while making use of the convolution theorem as well as the function $G_{l,m,n}(c,t)$ [11], when the application of the Inverse Laplace transform on eq.(22) is done, a demonstration of the velocity field unfolds as follows:

$$\begin{aligned}v(r,t) =& \frac{R_1(R_2^2-r^2)}{(R_2^2-R_1^2)r}\omega_1 \sin(\beta_1 t) + \frac{R_2(r^2-R_1^2)}{(R_2^2-R_1^2)r}\omega_2 \sin(\beta_2 t) + \pi \sum_{\gamma=1}^{\infty} \frac{J_1^2(R_1\kappa_\gamma)A_1(r\kappa_\gamma)}{J_1^2(R_1\kappa_\gamma)-J_1^2(R_2\kappa_\gamma)} \\ & \times \frac{1}{\lambda}\sum_{i=0}^{\infty}\sum_{q=0}^{i} \frac{i!}{q!(i-q)!}\left(-\frac{\nu\kappa_\gamma^2}{\lambda}\right)^i \lambda_r^q \int_0^t [\omega_1 \sin[\beta_1(t-\tau)]\frac{J_1(R_2\kappa_\gamma)}{J_1(R_1\kappa_\gamma)} \\ & -\omega_2 \sin[\beta_2(t-\tau)]]][G_{\alpha,\delta q-i,i+1}(-\lambda^{-1},\tau) + \lambda G_{\alpha,\delta q-i+\alpha,i+1}(-\lambda^{-1},\tau)]d\tau \\ & + \frac{\pi^2}{2}\sum_{\gamma=1}^{\infty} \frac{\kappa_\gamma J_1^2(R_1\kappa_\gamma)A_1(r\kappa_\gamma)}{J_1^2(R_1\kappa_\gamma)-J_1^2(R_2\kappa_\gamma)} \times \frac{1}{\lambda}\sum_{i=0}^{\infty}\sum_{q=0}^{i} \frac{i!}{q!(i-q)!}\left(-\frac{\nu\kappa_\gamma^2}{\lambda}\right)^i \lambda_r^q P_0[\overline{A_1}(R_1\kappa_\gamma)-\overline{A_1}(R_2\kappa_\gamma)] \\ & \int_0^t [\sin[\omega(t-\tau)]][G_{\alpha,\delta q-i,i+1}(-\lambda^{-1},\tau) + \lambda G_{\alpha,\delta q-i+\alpha,i+1}(-\lambda^{-1},\tau)]d\tau\end{aligned} \tag{23}$$

Where

$$G_{d,e,f}(c,t) = \sum_{j=0}^{\infty} \frac{(f)_j c^j t^{(j+f)d-e-1}}{(\Gamma(j+f)d-e)j!}$$

G is the generalized function and $(f)_j$ is the Pochhammer polynomial given in [11].
If it is presumed that, in the absence of a pressure gradient, the motion is exhibited on account of oscillation in the outer cylinder while the inner cylinder remains stationary, the velocity's manifestation given in eq. (23) becomes the same as the solutions posited in [8].

5 Shear Stress

Putting Laplace transform in eq.(9) we obtain,

$$\overline{\tau}(r,s) = \frac{\mu(1+\lambda_r s^\delta)}{(1+\lambda s^\alpha)}\left(\frac{\partial}{\partial r} - \frac{1}{r}\right)\overline{v}(r,s) \tag{24}$$

Plugging eq. (22) in eq. (24), achieved equation is:

$$\begin{aligned}\overline{\tau}(r,s) =& \frac{\mu(1+\lambda_r s^\delta)}{(1+\lambda s^\alpha)}\frac{2R_1R_2}{(R_2^2-R_1^2)r^2}\left(\frac{R_1\omega_2\beta_2}{s^2+\beta_2^2} - \frac{R_2\omega_1\beta_1}{s^2+\beta_1^2}\right) \\ & + \mu\pi\sum_{\gamma=1}^{\infty}\frac{J_1^2(R_1\kappa_\gamma)[\frac{2}{r}A_1(r\kappa_\gamma)-\kappa_\gamma\overline{A_1}(r\kappa_\gamma]}{J_1^2(R_1\kappa_\gamma)-J_1^2(R_2\kappa_\gamma)}\left[\frac{\omega_2\beta_2}{s^2+\beta_2^2} - \frac{\omega_1\beta_1}{s^2+\beta_1^2}\frac{J_1(R_2\kappa_\gamma)}{J_1(R_1\kappa_\gamma)}\right] \\ & \times \frac{s(1+\lambda_r s^\delta)}{s+\lambda s^{\alpha+1}+\kappa_\gamma^2\nu+\kappa_\gamma^2\nu\lambda_r s^\delta} + \frac{\mu\pi}{2}\sum_{\gamma=1}^{\infty}\frac{\kappa_\gamma J_1^2(R_1\kappa_\gamma)[\frac{2}{r}A_1(r\kappa_\gamma)-\kappa_\gamma\overline{A_1}(r\kappa_\gamma)]}{J_1^2(R_1\kappa_\gamma)-J_1^2(R_2\kappa_\gamma)} \\ & \frac{\rho P_0\omega[\overline{A_1}(R_1\kappa_\gamma)-\overline{A_1}(R_2\kappa_\gamma)]}{(s^2+\omega^2)} \times \frac{(1+\lambda_r s^\delta)}{s+\lambda s^{\alpha+1}+\kappa_\gamma^2\nu+\kappa_\gamma^2\nu\lambda_r s^\delta}\end{aligned} \tag{25}$$

Similarly, taking assistance of the generalized R function [17], the equation provided hereinafter is procured,

$$\begin{aligned}
\tau(r,t) =& \frac{2R_1R_2}{\lambda(R_2^2-R_1^2)r^2}\int_0^t [R_1\omega_2\sin\beta_2(t-\tau)-R_2\omega_1\sin\beta_1(t-\tau)][R_{\alpha,0}(-\lambda_{-1},t)+\lambda_r R_{\alpha,\delta}(-\lambda_{-1},t)]d\tau \\
&+\frac{\mu\pi}{\lambda}\sum_{\gamma=1}^{\infty}\frac{J_1^2(R_1\kappa_\gamma)[\frac{2}{r}A_1(r\kappa_\gamma)-\kappa_\gamma\overline{A_1}(r\kappa_\gamma]}{J_1^2(R_1\kappa_\gamma)-J_1^2(R_2\kappa_\gamma)}\times\frac{1}{\lambda}\sum_{i=0}^{\infty}\sum_{q=0}^{i}\frac{i!}{q!(i-q)!}\left(-\frac{\nu\kappa_\gamma^2}{\lambda}\right)^i\lambda_r^q \\
&\int_0^t[\omega_2\sin[\beta_2(t-\tau)]-\omega_1\sin[\beta_1(t-\tau)]\frac{J_1(R_2\kappa_\gamma)}{J_1(R_1\kappa_\gamma)}] \\
&[G_{\alpha,\delta q-i,i+1}(-\lambda^{-1},\tau)+\lambda_r G_{\alpha,\delta q+\delta-i,i+1}(-\lambda^{-1},\tau)]d\tau-\frac{\mu\pi}{2\lambda}\sum_{\gamma=1}^{\infty}\frac{J_1^2(R_1\kappa_\gamma)[\frac{2}{r}A_1(r\kappa_\gamma)-\kappa_\gamma\overline{A_1}(r\kappa_\gamma)]}{J_1^2(R_1\kappa_\gamma)-J_1^2(R_2\kappa_\gamma)} \\
&\frac{1}{\lambda}\sum_{i=0}^{\infty}\sum_{q=0}^{i}\frac{i!}{q!(i-q)!}\left(-\frac{\nu\kappa_\gamma^2}{\lambda}\right)^i\lambda_r^q\kappa_\gamma P_0[\overline{A_1}(R_1\kappa_\gamma)-\overline{A_1}(R_2\kappa_\gamma)] \\
&\times\int_0^t[\sin[\omega(t-\tau)]][G_{\alpha,\delta q-i,i+1}(-\lambda^{-1},\tau)+\lambda_r G_{\alpha,\delta q-i+\alpha,i+1}(-\lambda^{-1},\tau)]d\tau
\end{aligned} \tag{26}$$

where

$$R_{l,m}(c,t)=\sum_{j=0}^{\infty}\frac{c^j t^{(j+1)m-l-1}}{\Gamma[(j+1)l-m]}$$

During the course of the oscillation in the outer cylinder, where the inner cylinder is considered stationary, whereas the pressure gradient is absent, the shear stress' equation in eq. (26) conforms with the previous results given in Shin and Kang 2016 [8].

6 Results and Discussions

The analytical solution for the velocity profile and shear stress for the flow of fractionalized Oldroyd-B fluid in oscillating coaxial cylinders is investigated using Caputo fractional differential operator, and integral transform; (i.e Laplace transform and the Finite Hankel transform). Cylinders are initially at rest and as the cylinders start oscillating, the fluid moves due to the applied oscillating pressure gradient. In this work, we investigated the impact of several parameters, including the amplitude ω_1 and ω_2, frequencies β_1, β_2, time relaxation λ, time retardatione λ_r, the kinematic viscosity ν, and the fractional parameter α. The consequences of these variables on the velocity of the fluid and shear stress are defined in eq. (23) and eq.(26) correspondingly. Entire figures are used in SI unit and the roots are estimated by $\kappa_\gamma = \frac{(2n-1)\pi}{(R_2-R_1)}$. To validate the physical appearance of the results achieved in different situations, graphical depictions of the velocity profile and the stress were generated for different values of t and substantial parameters, against r via Mathematica 7. The impact of time on the momentum of fluid is exemplified in Fig. 2, which shows that the velocity is decreasing whereas the shear stress is spotted to increase with increasing time. Oscillation of the cylinders enhances the velocity of the fluid at the inlet, however, it decreases as the fluid travels towards an exit. Fig 3 demonstrates that increasing the oscillation of the inner cylinder β_1 fixing β_2 = 1 ms^{-1}, the velocity of the fluid drops with decreasing the absolute value of shear stress. However, the contrary behaviour is noticed for the oscillation of an outer cylinder which is depicted in Fig 4. The trends show increasing behaviours initially and then at r = 0.47 m, it drops suddenly due to the oscillating pressure gradient. Furthermore, Fig 5 clarifies the effect of amplitude and explains that the inner cylinder *omega*$_1$ enhances the fluid's velocity whilst reducing the shear stress. The and stress and the velocity profile also enhances the amplitude of the outer cylinder ω_2 and is described in Fig 6. The converse correlation between kinematic viscosity and velocity due to the oscillating pressure gradient is discussed in Fig 7, which indicates that the more the viscous fluid, the less velocity and more shear stress is required. The result validates the physics that shows the fact that increasing the viscosity proposes aversion in the fluid, that lessens the velocity. Fig. 8 reveals impact of the relaxation parameter λ, which shows that increasing the λ, enhances the stress and the velocity profile. This can be accredited to viscous effects become fragile with an increase in the λ. Fig. 9 states that the effect of time retardation λ_r has inverse behaviour on the fluid. Lastly, significance of the parameter of the fractional operator is depicted in fig. 10. It can be noticed, by intensifying the value of α the velocity enhances and the shear stress drops. For entire parameters, we can notice the higher fluid velocity at the inner cylinder, however, it reduces as it flows to the outer cylinder. The coherence in the results is observed for several parameters and the graphical demonstration is in good agreement with the previous work investigated [12].

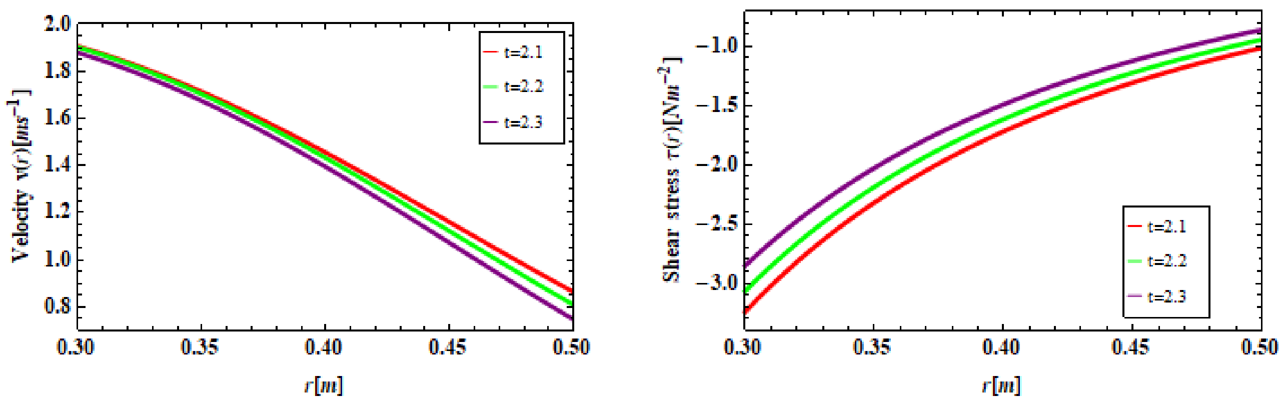

Figure 2. Velocity profile and Shear stress for numerous values of t with $R_1 = \frac{3}{10}$,$R_2 = \frac{1}{2}$,$\omega_1 = 1.0$, $\omega_2 = 1.0$, $\beta_1 = 1.0$, $\beta_2 = 1.0$, $\omega = 1.0$, $\lambda = 4.0$, $\lambda_r = 2.0$, $\nu = 0.55660$, $\mu = 1.01$, $p_0 = 0.420$, $\delta = \frac{1}{2}$ and $\alpha = \frac{4}{5}$.

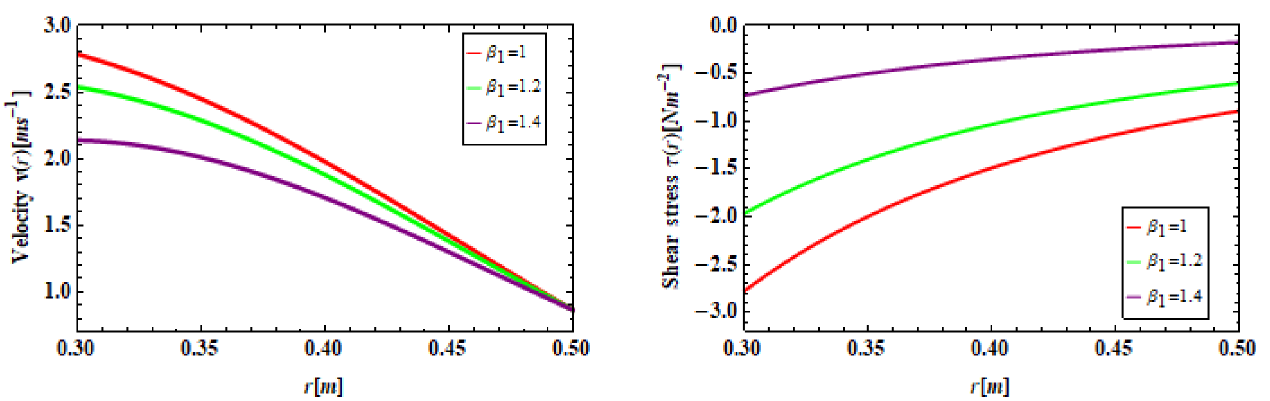

Figure 3. Velocity profile and Shear stress for numerous values of β_1 with $R_1 = \frac{3}{10}$,$R_2 = \frac{1}{2}$,$\omega_1 = 1.0$, $\omega_2 = 1.0$, $t = t = \frac{21}{10}$, $\beta_2 = 1.0$, $\omega = 1.0$, $\lambda = 4.0$, $\lambda_r = 2.0$, $\nu = 0.55660$, $\mu = 1.01$,$p_0 = 0.420$, $\delta = \frac{1}{2}$, and $\alpha = \frac{4}{5}$.

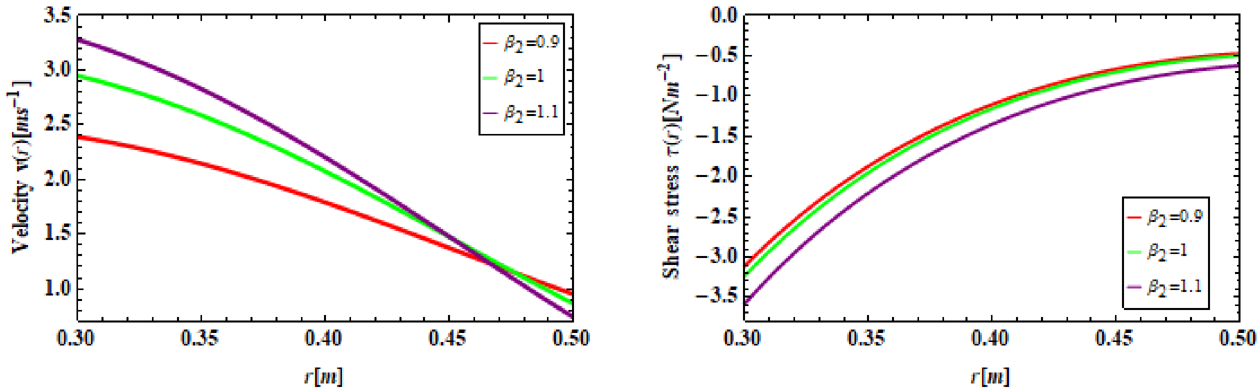

Figure 4. Velocity profile and shear stress for numerous values of β_2 with $R_1 = \frac{3}{10}$,$R_2 = \frac{1}{2}$,$\omega_1 = 1.0$, $\omega_2 = 1.0$, $\beta_1 = 1.0$, $t = t = \frac{21}{10}$, $\omega = 1.0$, $\lambda = 4.0$, $\lambda_r = 2.0$, $\nu = 0.55660$, $\mu = 1.01$ $p_0 = 0.420$, $\delta = \frac{1}{2}$, and $\alpha = \frac{4}{5}$.

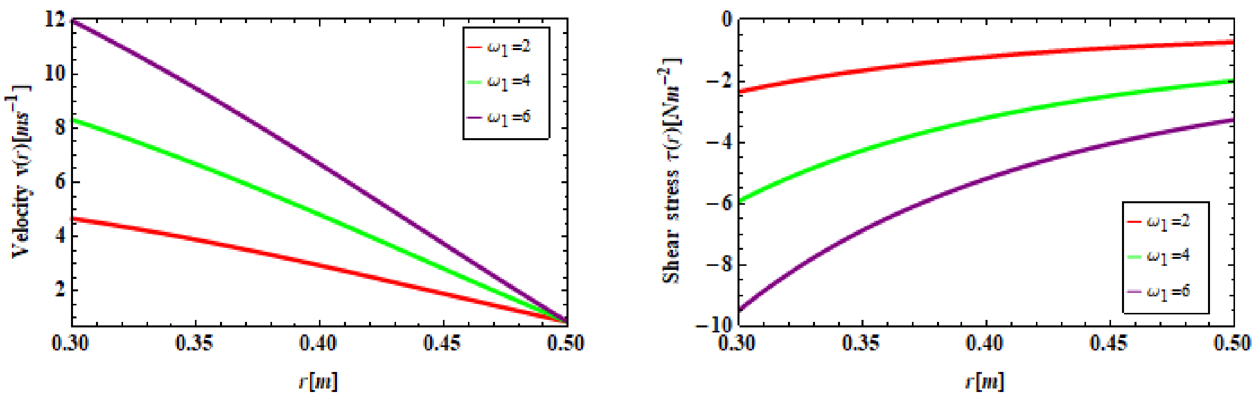

Figure 5. Velocity profile and Shear stress for numerous values of ω_1 with $R_1 = \frac{3}{10}$,$R_2 = \frac{1}{2}$,$t = t = \frac{21}{10}$, $\omega_2 = 1.0$, $\beta_1 = 1.0$, $\beta_2 = 1.0$, $\omega = 1.0$, $\lambda = 4.0$, $\lambda_r = 2.0$, $\nu = 0.55660$, $\mu = 1.01$,$p_0 = 0.420$, $\delta = \frac{1}{2}$ and $\alpha = \frac{4}{5}$.

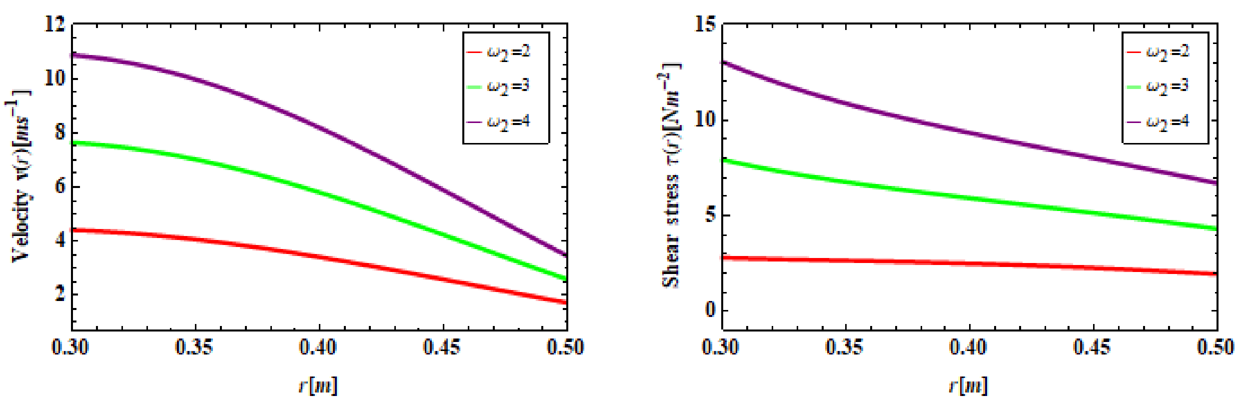

Figure 6. Velocity profile and Shear stress for numerous values of ω_2 with $R_1 = \frac{3}{10}$,$R_2 = \frac{1}{2}$,$t = t = \frac{21}{10}$, $\omega_2 = 1.0$, $\beta_1 = 1.0$, $\beta_2 = 1.0$, $\omega = 1.0$, $\lambda = 4.0$, $\lambda_r = 2.0$, $\nu = 0.55660$, $\mu = 1.01$,$p_0 = 0.420$, $\delta = \frac{1}{2}$, and $\alpha = \frac{4}{5}$.

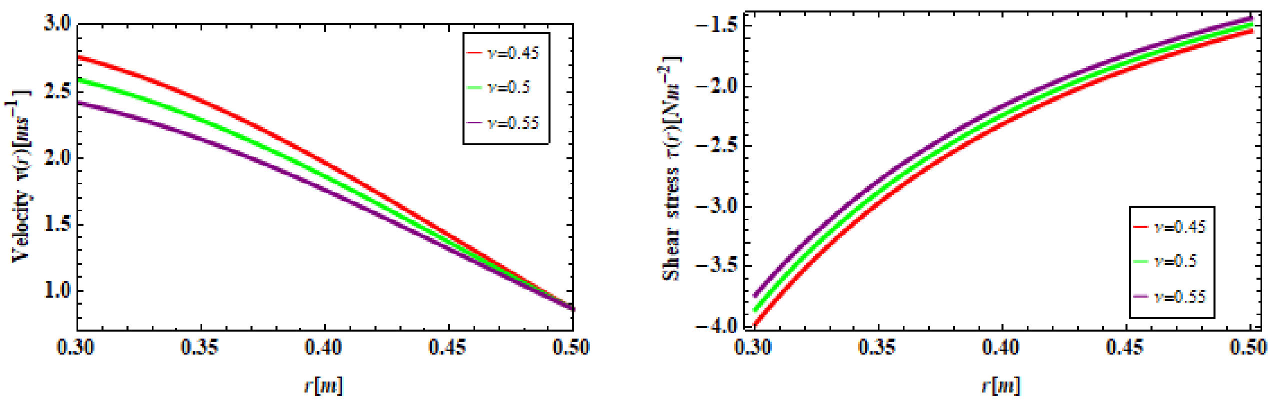

Figure 7. Velocity profile and Shear stress for numerous values of ν with $R_1 = \frac{3}{10}$,$R_2 = \frac{1}{2}$,ω_1.0 = 1, ω_2 = 1.0, β_1 = 1.0, β_2 = 1.0, ω = 1.0, λ = 4.0, λ_r = 2.0, $t = t = \frac{21}{10}$, μ = 1.01, p_0 = 0.420, $\delta = \frac{1}{2}$, and $\alpha = \frac{4}{5}$.

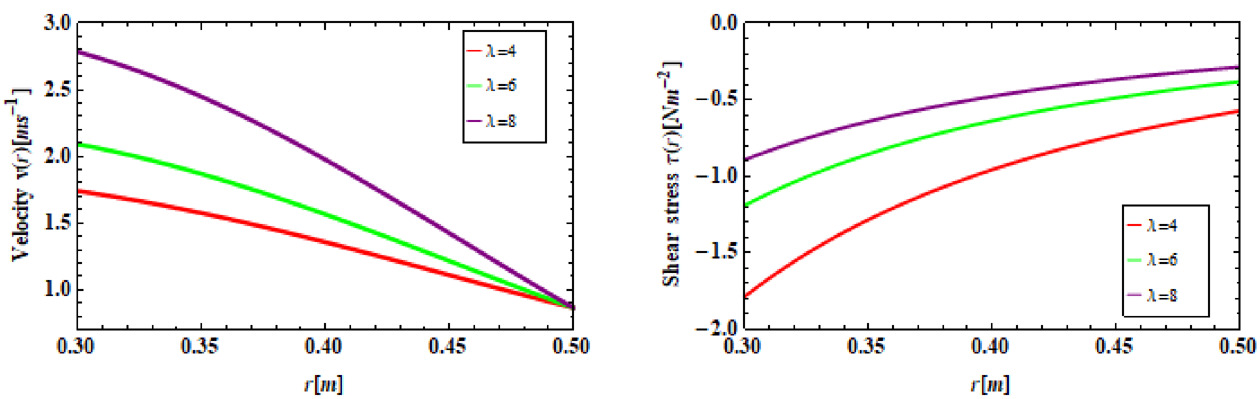

Figure 8. Velocity profile and Shear stress for numerous values of λ with $R_1 = \frac{3}{10}$,$R_2 = \frac{1}{2}$,ω_1 = 1.0, ω_2 = 1.0, β_1 = 1.0, β_2 = 1.0, ω = 1.0, $t = t = \frac{21}{10}$, λ_r = 2.0, ν = 0.55660, μ = 1.01,p_0 = 0.420, $\delta = \frac{1}{2}$, and $\alpha = \frac{4}{5}$.

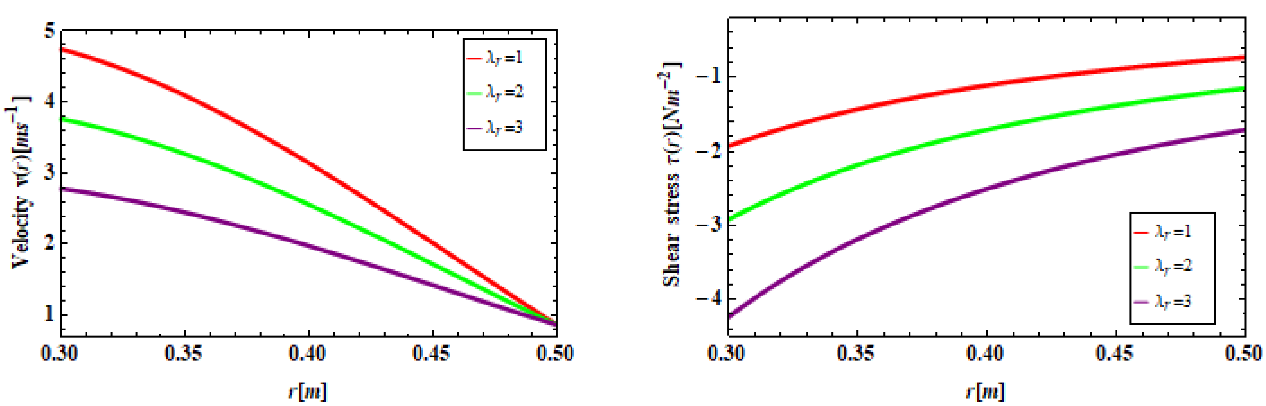

Figure 9. Velocity profile and Shear stress for numerous values of λ_r with $R_1 = \frac{3}{10}$,$R_2 = \frac{1}{2}$,ω_1 = 1.0, ω_2 = 1.0, β_1 = 1.0, β_2 = 1.0, ω = 1.0, λ = 4.0, $t = t = \frac{21}{10}$, ν = 0.55660, μ = 1.01,p_0 = 0.420, $\delta = \frac{1}{2}$ and $\alpha = \frac{4}{5}$.

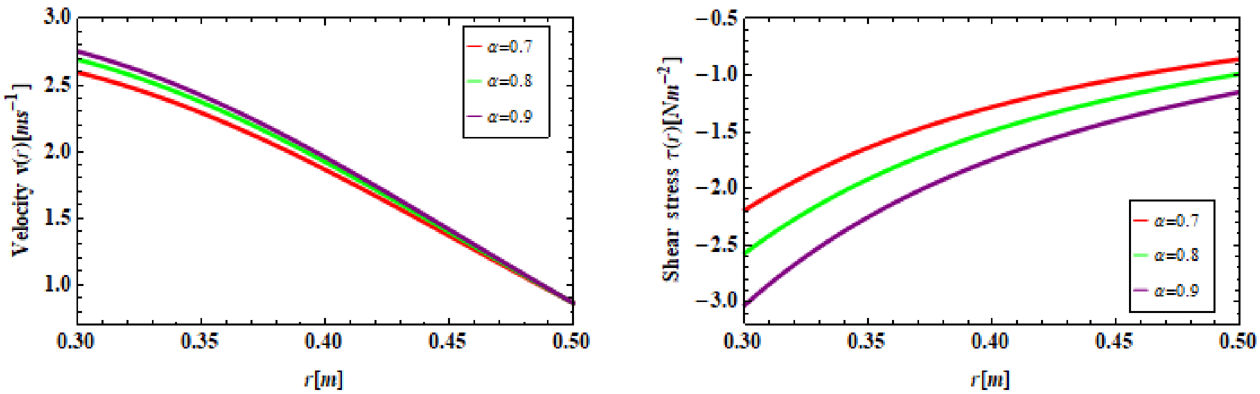

Figure 10. Velocity profile and Shear stress for numerous values of α with $R_1 = \frac{3}{10}$,$R_2 = \frac{1}{2}$,$\omega_1 = 1.0$, $\omega_2 = 1.0$, $\beta_1 = 1.0$, $\beta_2 = 1.0$, $\omega = 1.0$, $\lambda = 4.0$, $\lambda_r = 2.0$, $\nu = 0.55660$, $\mu = 1.01$, $p_0 = 0.420$, $\delta = \frac{1}{2}$, and $t = \frac{21}{10}$.

7 Discussion and conclusions

In the current research work, the articulation for the stress and the velocity distribution of fractionalized Oldroyd-B fluid utilizing the caputo operator with integral tranforms are achieved. The movement of the fluid is assumed to be oscillating due to cylinders oscillation and also the oscillating pressure gradient. The results are proposed are in series and integral form of R and G functions. The constitutive equations and the corresponding conditions(i.e, initial and boundary conditions) are identically satisfied.

- The motion of fluid exhibits comparatively more acceleration at the inlet of the cylinder than at the outlet.
- The velocity of fluid experiences decline while escalation is manifested in shear stress (absolute values) with time.
- The influence of β_1 and β_2 on fluid's velocity and shear stress show opposite behavior.
- The amplitude of the inner cylinder and outer cylinder, i.e ω_1 and ω_2, have an analogous effect on the velocity and shear stress of fluid.
- The kinematic viscosity's value is directly proportional to the value of shear stress, however, it is inversely proportional to the pace of velocity.
- The effects of both non-Newtonian parameters, i.e λ and λ_r, manifest opposite results on the fluid's motion.
- The velocity and shear stress (in absolute values) are increasing functions of fractional parameters.

Author Contributions

Khadija Shaikh: Methodology, Software, Writing- Original draft preparation. **Fozia Shaikh**: Conceptualization, Visualization **Syed Feroz Shah**: Supervision. **Rahim Bux Khokhar**:Reviewing and Editing : **K.N. Memon**:Writing and Validation.

Compliance with Ethical Standards

The authors claim to have no conflicts of interest.

Funding Information

In the course of conducting this research, no funding was received.

Author Information

ORCID:

Fozia Shaikh: 0000-0002-1049-5268

References

[1] Alam, M. K., Memon, K., Siddiqui, A., Shah, S., Farooq, M., Ayaz, M., Nofal, T. A. and Ahmad, H. [2021], 'Modeling and analysis of high shear viscoelastic ellis thin liquid film phenomena', *Physica Scripta* **96**(5), 055201.

[2] Ali Zafar, A., Bilal Riaz, M. and Imran Asjad, M. [2020], 'Unsteady rotational flow of fractional maxwell fluid in a cylinder subject to shear stress on the boundary', *Punjab University Journal of Mathematics* **50**(2).

[3] Armstrong, R. C. and Hassager, O. [1987], *Dynamics of polymeric liquids: Fluid mechanics*, Wiley.

[4] Debnath, L. and Bhatta, D. [2016], *Integral transforms and their applications*, Chapman and Hall/CRC.

[5] Fetecau, C., Fetecau, C., Jamil, M. and Mahmood, A. [2011], 'Retracted article: Flow of fractional maxwell fluid between coaxial cylinders', *Archive of Applied Mechanics* **81**(8), 1153–1163.

[6] Haitao, Q. and Mingyu, X. [2009], 'Some unsteady unidirectional flows of a generalized oldroyd-b fluid with fractional derivative', *Applied Mathematical Modelling* **33**(11), 4184–4191.

[7] Kamran, M., Athar, M. and Imran, M. [2012], 'Critical study on rotational flow of a fractional oldroyd-b fluid induced by a circular cylinder', *International Scholarly Research Notices* **2012**.

[8] Kang, S. M., Nazeer, W., Athar, M., Hisham, M. D. and Kwun, Y. C. [2016], 'Retracted article: Velocity and shear stress for an oldroyd-b fluid within two cylinders', *Boundary Value Problems* **2016**(1), 1–11.

[9] Khalique, C. M., Safdar, R. and Tahir, M. [2019], 'First analytic solution for the oscillatory flow of a maxwells fluid with annulus', *Open Journal of Mathematical Sciences* **2**, 1–9.

[10] Khaskheli, M. A., Memon, K. N., Sheikh, A. H., Siddiqui, A. M. and Shah, S. F. [2020], 'Tank drainage for an electrically conducting newtonian fluid with the use of the bessel function', *Eng. Technol. Appl. Sci. Res* **10**(2).

[11] Lorenzo, C. F. and Hartley, T. T. [2008], 'Generalized functions for the fractional calculus', *Critical Reviews™ in Biomedical Engineering* **36**(1).

[12] Mathur, V. and Khandelwal, K. [2017], 'Flow of fractional maxwell fluid in oscillating pipe-like domains', *International Journal of Applied and Computational Mathematics* **3**(2), 841–858.

[13] Memon, K. N., Alam, M. K., Baili, J., Nawaz, Z., Shiekh, A. H. and Ahmad, H. [2021], 'Analytical solution of tank drainage flow for electrically conducting newtonian fluid', *Thermal Science* **25**(Spec. issue 2), 433–439.

[14] Qi, H. and Jin, H. [2009], 'Unsteady helical flows of a generalized oldroyd-b fluid with fractional derivative', *Nonlinear analysis: real world applications* **10**(5), 2700–2708.

[15] Qureshi, S. and Kumar, P. [2019], 'Using shehu integral transform to solve fractional order caputo type initial value problems', *Journal of Applied Mathematics and Computational Mechanics* **18**(2).

[16] Rauf, A., Rubbab, Q., Vieru, D. and Majeed, A. [2020], 'Simultaneous flow of two immiscible fractional maxwell fluids with the clear region and homogeneous porous medium', *Sains Malaysiana* **49**(11), 2871–2880.

[17] Sadiq, N., Imran, M., Safdar, R., Tahir, M., Javaid, M. and Younas, M. [2020], 'Exact solution for some rotational motions of fractional oldroyd-b fluids between circular cylinders', *Punjab University Journal of Mathematics* **50**(4).

[18] Shah, S. A. R., Memon, K., Shah, S., Sheikh, A. and Siddiqui, A. [2022], 'Delta perturbation method for thin film flow of a third grade fluid on a vertical moving belt', *STATISTICS, COMPUTING AND INTERDISCIPLINARY RESEARCH* **4**(1), 61–73.

[19] Shaikh, F., Shah, S. F., Siddiqui, A. and Kumar, L. [2022], 'Application of recursive approach of pseudoplastic fluid flow between rotating coaxial cylinders', *Alexandria Engineering Journal* **61**(10), 7823–7832.

[20] Syam, M. and Al-Refai, M. [2019], 'Fractional differential equations with atangana–baleanu fractional derivative: analysis and applications', *Chaos, Solitons & Fractals: X* **2**, 100013.

[21] Tahir, M., Naeem, M. N., Javaid, M., Younas, M., Imran, M., Sadiq, N. and Safdar, R. [2018], 'Unsteady flow of fractional oldroyd-b fluids through rotating annulus', *Open Physics* **16**(1), 193–200.

[22] Wang, F. and Liu, J. [2020], 'The first solution for the helical flow of a generalized maxwell fluid within annulus of cylinders by new definition of transcendental function', *Mathematical Problems in Engineering* **2020**.

[23] Wang, F., Shen, W.-C., Liu, J.-L. and Wang, P. [2020], 'The analytic solutions for the unsteady rotating flows of the generalized maxwell fluid between coaxial cylinders', *Thermal Science* **24**(6 Part B), 4041–4048.

[24] Yang, X.-J., Gao, F. and Yang, J. [2020], *General fractional derivatives with applications in viscoelasticity*, Academic Press.

[25] Zafar, A., Riaz, M., Shah, N. and Imran, M. [2018], 'Influence of non-integer-order derivatives on unsteady unidirectional motions of an oldroyd-b fluid with generalized boundary conditions', *The European Physical Journal Plus* **133**(3), 1–13.